

Electronic Supporting Information

A novel Pt-Co alloy hydrogen anode catalyst with superlative activity, CO-tolerance and robustness

Guoyu Shi,^a Hiroshi Yano,^b Donald A. Tryk,^b Masahiro Watanabe,^b Akihiro Iiyama,^b

and Hiroyuki Uchida^{*b, c}

^aInterdisciplinary Graduate School of Medicine and Engineering, University of Yamanashi, Takeda 4, Kofu, 400 8510, Japan

^bFuel Cell Nanomaterials Center, University of Yamanashi, Takeda 4, Kofu, 400-8510, Japan

^cClean Energy Research Center, University of Yamanashi, Takeda 4, Kofu, 400-8510, Japan

E-mail: h-uchida@yamanashi.ac.jp; Fax: +81-55-220-8618; Tel: +81-55-220-8619

Contents

1. Experimental procedures

2. Theoretical calculation methods

3. References

4. Figures

Figure S1. TEM images and particle size distribution histograms of the catalysts.

Figure S2. Hydrodynamic voltammograms for the CO-tolerant HOR.

Figure S3. CO-poisoning time dependence of apparent mass activity, MA_{app} .

Figure S4. Pt(110) unit cells with adsorbed CO and H₂.

Figure S5. Cross-sectional views of unit cells with adsorbed CO and H₂.

1. Experimental procedures

The working electrode consisted of c-Pt/C (46.1 wt%-Pt), c-Pt₃Co/C (46.4 wt%-Pt, 5.0 wt%-Co), Pt_{2AL}-PtCo/C (28.5 wt%-Pt, 4.2 wt%-Co), and c-Pt₂Ru₃/C (29.8 wt%-Pt, 23.2 wt%-Ru) catalysts dispersed uniformly on an Au substrate electrode (flow direction length 1 mm × width 4 mm) at a constant loading of carbon support, 11.0 μg cm⁻², which corresponds to approximately two monolayers in height of the carbon black particles.¹⁻³ An aliquot of 0.2 wt% Nafion (diluted with a mixture of ethanol and water at 3:2 v/v) solution was pipetted onto the catalyst layer to yield an average film thickness of 0.075 μm. The Nafion-coated electrode was dried under ethanol vapor pressure at room temperature. Finally, the Nafion-coated electrode was heated at 130°C for 30 min in air.

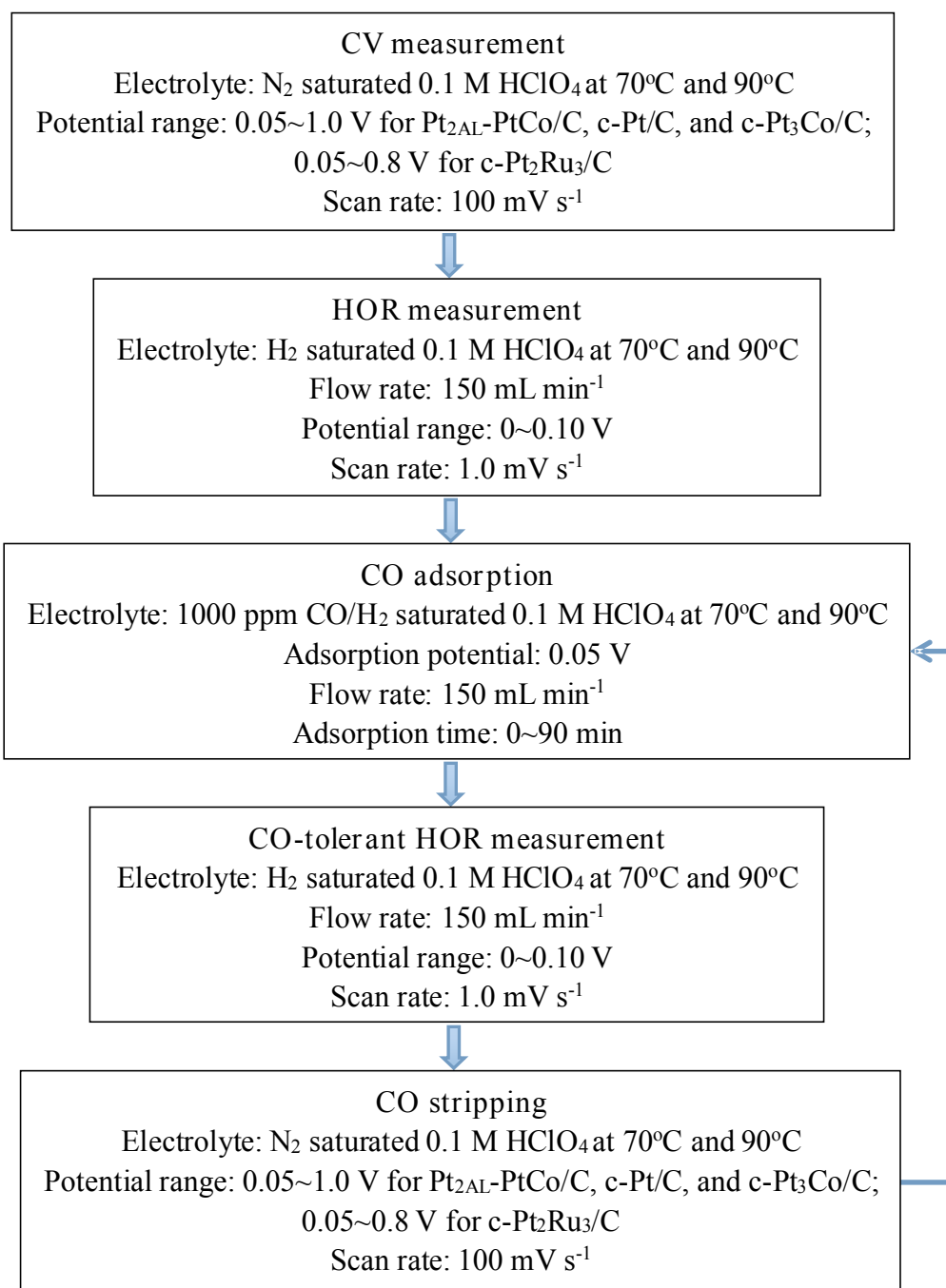
A platinum wire was used as the counter electrode. A reversible hydrogen electrode RHE(*t*), maintained at the same temperature as that of the cell, was used as the reference electrode. All the electrode potentials in this paper will be referenced to the RHE(*t*). The electrolyte solution, 0.1 M HClO₄, was prepared from reagent grade chemicals (Kanto Chemical Co.) and Milli-Q water, and purified in advance with conventional pre-electrolysis methods.^{4,5} The electrolyte solution was saturated with N₂, pure H₂, and CO-containing H₂ (1000 ppm CO, Sumitomo Seika, Japan) bubbling in three separate Teflon reservoirs, respectively, for at least 1 h prior to the electrochemical measurements.

A potentiostat (ALS 700A, BAS Inc.) was used for the electrochemical measurements. Prior to the HOR experiments at each temperature, the working electrode was electrochemically stabilized by repetitive sweeping the potential from 0.05 to 1.00 V for c-Pt/C, c-Pt₃Co/C, and Pt_{2AL}-PtCo/C, and from 0.05 to 0.80 V for c-Pt₂Ru₃/C at a sweep rate of 0.50 V s⁻¹ in 0.1 M HClO₄ solution deaerated with N₂ gas at 70°C until the voltammogram reached a steady state (typically 20 cycles). Then the CO-tolerant HOR activity was measured by using the following protocol (Scheme S1). The CO coverage (θ_{CO}) as the site occupation was determined by the CO-stripping voltammogram. The calculation is based on the following equation, regardless of the type of CO_{ad}, e.g., linear (on-top), bridged, or the derivatives,

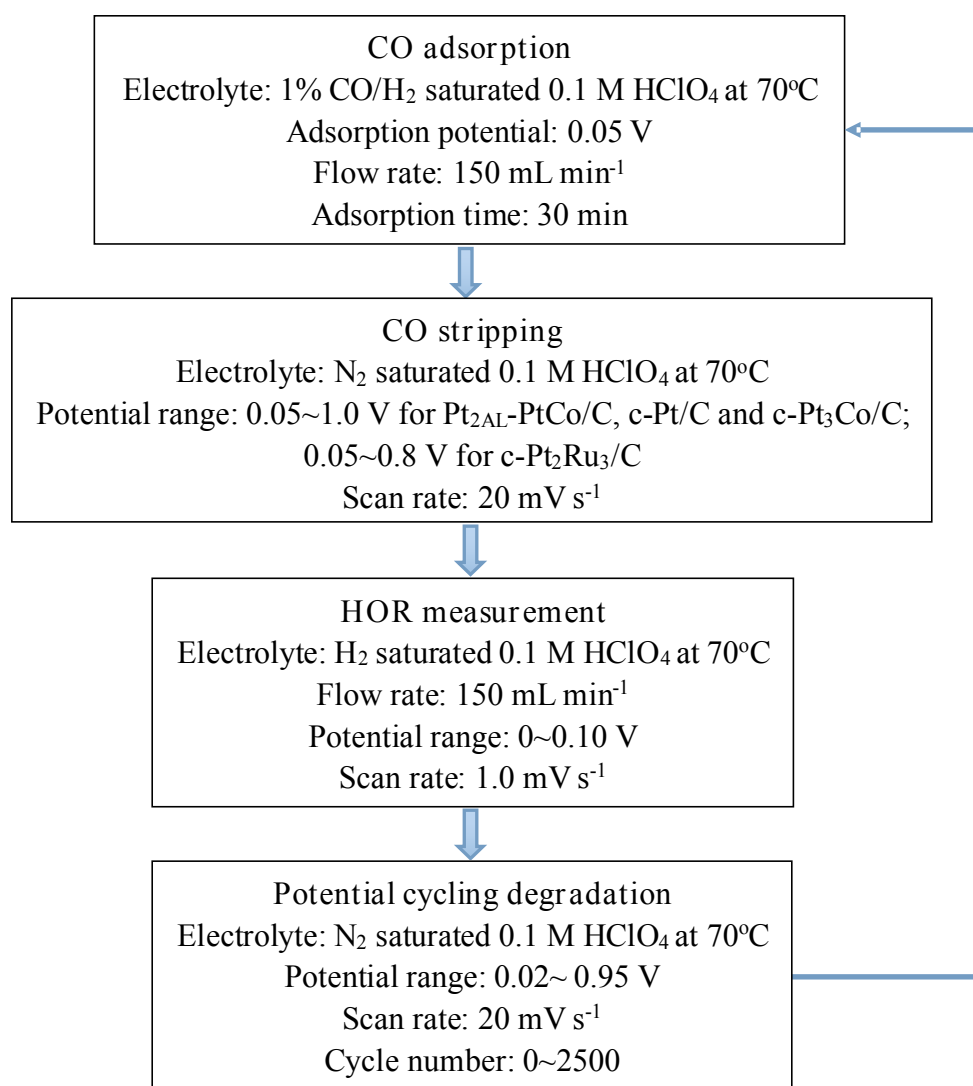
$$\theta_{\text{CO}} = 1 - (\Delta Q_{\text{H}} / \Delta Q_{\text{H}}^{\circ}) \quad (1)$$

where ΔQ_{H} and $\Delta Q_{\text{H}}^{\circ}$ are the hydrogen-desorption charges with and without CO_{ad}, respectively.⁶

Finally, the HOR durability test was carried out by potential cycling (0.02-0.95 V) at 20 mV s⁻¹ in N₂-saturated 0.1 M HClO₄ at 70°C, as shown in Scheme S2. After 2500 cycles, the HOR activity after 30 min CO-poisoning in 1000 ppm CO/H₂ was examined by using the protocol as described in Scheme S1.



Scheme S1. The experimental protocol for measuring the CO-tolerant HOR activity.



Scheme S2. Experimental protocol for measuring the catalyst durability that simulates the repeated exposure of the fuel cell anode to reformat gas and air during daily start/stop cycles.

2. Theoretical Calculation Methods

In order to obtain reliable estimates of adsorption energies for carbon monoxide and atomic hydrogen, it is necessary to make use of high-accuracy electronic structure density function theoretical (DFT) calculations, taking into account relativistic effects. Using such calculations, it has been shown to be possible to achieve good agreement between experiment and theory, for carbon monoxide on Pt(111)⁷ and atomic hydrogen on various Pt(hkl) surfaces.⁸⁻¹¹ In the present work, as in the work cited,⁷⁻¹¹ the DFT calculations were carried out with the DMol³ software package (BIOVIA, Materials Studio, Version 7.0).¹² The finest settings were used for the geometric optimization (convergence criteria, 1×10^{-5} Ha, maximum force 0.002 Ha/Å, maximum displacement 0.005 Å), which was carried out with density functional semicore pseudopotentials,¹³ with a double-numeric quality basis set with polarization

functions (dnp), and the final energies were calculated with all-electron scalar relativistic corrections. The gradient-corrected GGA functional used was developed by Perdew, Burke and Ernzerhof (pbe).¹⁴ To facilitate scf convergence, kinetic energy was applied to the electrons (thermal smearing) of 0.005 Ha for Pt(110) and 0.003 Ha for the Pt-Co alloys.

Periodic boundary conditions (PBC) were used, with three layers of metal atoms (Pt and/or Co) and a surface mesh of 4×4, shown for Pt(110) (Figure S4) and Pt₃Co. For the latter, half of the atoms in the troughs of the top layer were converted from Co to Pt to simulate the formation of a Pt skin layer. To simulate the Pt_{2AL}-PtCo(110) surface, with its higher concentration of Co close to the surface, half of the atoms below the Pt ridge atoms in the Pt-skin/Pt₃Co(110) structure were converted from Pt to Co.

For pure Pt, the lattice parameter used for the face-centered cubic (fcc) structure was the standard experimental bulk value of 3.93 Å; for Pt₃Co, the fcc lattice parameter was 3.831 Å (space group Pm-3m);¹⁵ For all of these structures, the xyz coordinates of the 8 bottom layer atoms were constrained to conform to those of the bulk structure.

The cross-sectional views for the Pt(110), Pt skin/Pt₃Co(110) with Co-enriched underlayer (to simulate Pt_{2AL}-PtCo(110)), Pt skin/Pt₃Co(110) with Co in the second layer, and Pt skin/Pt₃Co(110) with Pt in the second layer are shown in Figure S5. These structures correspond to those shown in Figure 2 in the main text.

Table S1. Adsorption energies (eV) for H, H₂ and CO on various surfaces.

Surface	H(calc.)	H(exp.)	H ₂ (calc.)	CO-top(calc.)	CO-top(exp.)	CO-br(calc.)
Pt(110)	-2.928	-2.798 ^a	-1.313	-2.345	-1.897 ^b	-2.340
Pt _{2AL} -PtCo(110)	-	-	-1.048	-1.992	-	-2.129
Pt ₃ Co(110)-Co _{UL} ^c	-	-	-1.070	-2.137	-	-2.429
Pt ₃ Co(110)-Pt _{UL} ^c	-	-	-1.565	-2.485	-	-2.429

^aRef. 16.

^bRef. 17.

^cUL denotes the type of atom in the second layer or underlayer beneath the top layer Pt at which adsorption occurs.

The results for H, H₂ and CO adsorption strengths at a coverage of 1/8 are shown in Table S1. The experimental values cited are for low coverage limits. The agreement between calculated values and experimental values is quite good for H on Pt(110), but the calculated value for CO is substantially higher than the experimental one, as noted earlier by Yamagishi et al.;¹⁸ for comparison, their calculated value, also using DMol³,

as in the present work, for CO adsorption energy on Pt(110) was -2.55 eV at 1/8 monolayer coverage, compared to -2.345 eV obtained in the present work. It should also be noted that the same group obtained a calculated value for atop CO adsorption on Pt(111) (-1.94 eV) that was only slightly higher than the experimental value of -1.90 eV, agreement that helps to increase the confidence in the DMol³ calculations.⁷

3. References

- (1) Higuchi, E.; Uchida, H.; Watanabe, M. Effect of Loading Level in Platinum-Dispersed Carbon Black Electrocatalysts on Oxygen Reduction Activity Evaluated by Rotating Disk Electrode. *J. Electroanal. Chem.* **2005**, *583*, 69-76.
- (2) Yano, H.; Higuchi, E.; Uchida, H.; Watanabe, M. Temperature Dependence of Oxygen Reduction Activity at Nafion-Coated Bulk Pt and Pt/Carbon Black Catalysts. *J. Phys. Chem. B* **2006**, *110*, 16544-16549.
- (3) Yano, H.; Inukai, J.; Uchida, H.; Watanabe, M.; Panakkattu, K. B.; Kobayashi, T.; Chung, J. H.; Oldfield, E.; Wieckowski, A. Particle-Size Effect of Nanoscale Platinum Catalysts in Oxygen Reduction Reaction: An Electrochemical and 195 Pt EC-NMR Study. *Phys. Chem. Chem. Phys.* **2006**, *8*, 4932-4939.
- (4) Watanabe, M.; Motoo, S. Electrocatalysis by Ad-Atoms: Part I. Enhancement of the Oxidation of Methanol on Platinum and Palladium by Gold Ad-Atoms. *J. Electroanal. Chem.* **1975**, *60*, 259-266.
- (5) Uchida, H.; Ikeda, N.; Watanabe, M. Electrochemical Quartz Crystal Microbalance Study of Copper Adatoms on Gold Electrodes Part II. Further Discussion on the Specific Adsorption of Anions from Solutions of Perchloric and Sulfuric Acid. *J. Electroanal. Chem.* **1997**, *424*, 5-12.
- (6) Uchida, H.; Izumi, K.; Aoki, K.; Watanabe, M. Temperature-Dependence of Hydrogen Oxidation Reaction Rates and CO-Tolerance at Carbon-Supported Pt, Pt-Co, and Pt-Ru Catalysts. *Phys. Chem. Chem. Phys.* **2009**, *11*, 1771-1779.
- (7) Orita, H.; Itoh, N.; Inada, Y. All Electron Scalar Relativistic Calculations on Adsorption of CO on Pt (111) with Full-Geometry Optimization: a Correct Estimation for CO Site-Preference. *Chem. Phys. Lett.* **2004**, *384*, 271-276.
- (8) Ishikawa, Y.; Mateo, J. J.; Tryk, D. A.; Cabrera, C. R. Direct Molecular Dynamics and Density-Functional Theoretical Study of the Electrochemical Hydrogen Oxidation Reaction and Underpotential Deposition of H on Pt (111). *J. Electroanal. Chem.* **2007**, *607*, 37-46.
- (9) Mateo, J. J.; Tryk, D. A.; Cabrera, C. R.; Ishikawa, Y. Underpotential Deposition of Hydrogen on Pt (111): a Combined Direct Molecular Dynamics/Density Functional Theory Study. *Mol. Simul.* **2008**, *34*, 1065-1072.
- (10) Santana, J. A.; Mateo, J. J.; Ishikawa, Y. Electrochemical Hydrogen Oxidation on Pt (110): a Combined Direct Molecular Dynamics/Density Functional Theory Study. *J. Phys. Chem. C* **2010**, *114*, 4995-5002.
- (11) Santana, J. A.; Saavedra-Arias, J. J.; Ishikawa, Y. Electrochemical Hydrogen Oxidation on Pt (100): a Combined Direct Molecular Dynamics/Density Functional Theory Study. *Electrocatal.* **2015**, *6*, 534-543.

- (12) Delley, B. A Scattering Theoretic Approach to Scalar Relativistic Corrections on Bonding. *Int. J. Quant. Chem.* **1998**, *69*, 423-433.
- (13) Delley, B. Hardness Conserving Semilocal Pseudopotentials. *Phys. Rev. B* **2002**, *66*, 155125.
- (14) Perdew, J. P.; Burke, K.; Ernzerhof, M. Generalized Gradient Approximation Made Simple. *Phys. Rev. Lett.* **1996**, *77*, 3865.
- (15) Geisler, A. H.; Martin, D. L. A New Superlattice in Co-Pt alloys. *J. Appl. Phys.* **1952**, *23*, 375.
- (16) Christmann, K. In *Electrocatalysis*; Lipkowski, J.; Ross, P. N., Eds.; Wiley-VCH: New York, **1998**.
- (17) Watanabe, C. E.; Stuck, A.; Yeo, Y. Y.; King, D. A. Microcalorimetric Heats of Adsorption for CO, NO, and Oxygen on Pt{110}. *J. Phys. Chem.* **1996**, *100*, 12483-12488.
- (18) Yamagishi, S.; Fujimoto, T.; Inada, Y.; Orita, H. Studies of CO Adsorption on Pt(100), Pt(410) and Pt(110) Surfaces Using Density Functional Theory. *J. Phys. Chem. B* **2005**, *109*, 8899-8908.

4. Figures

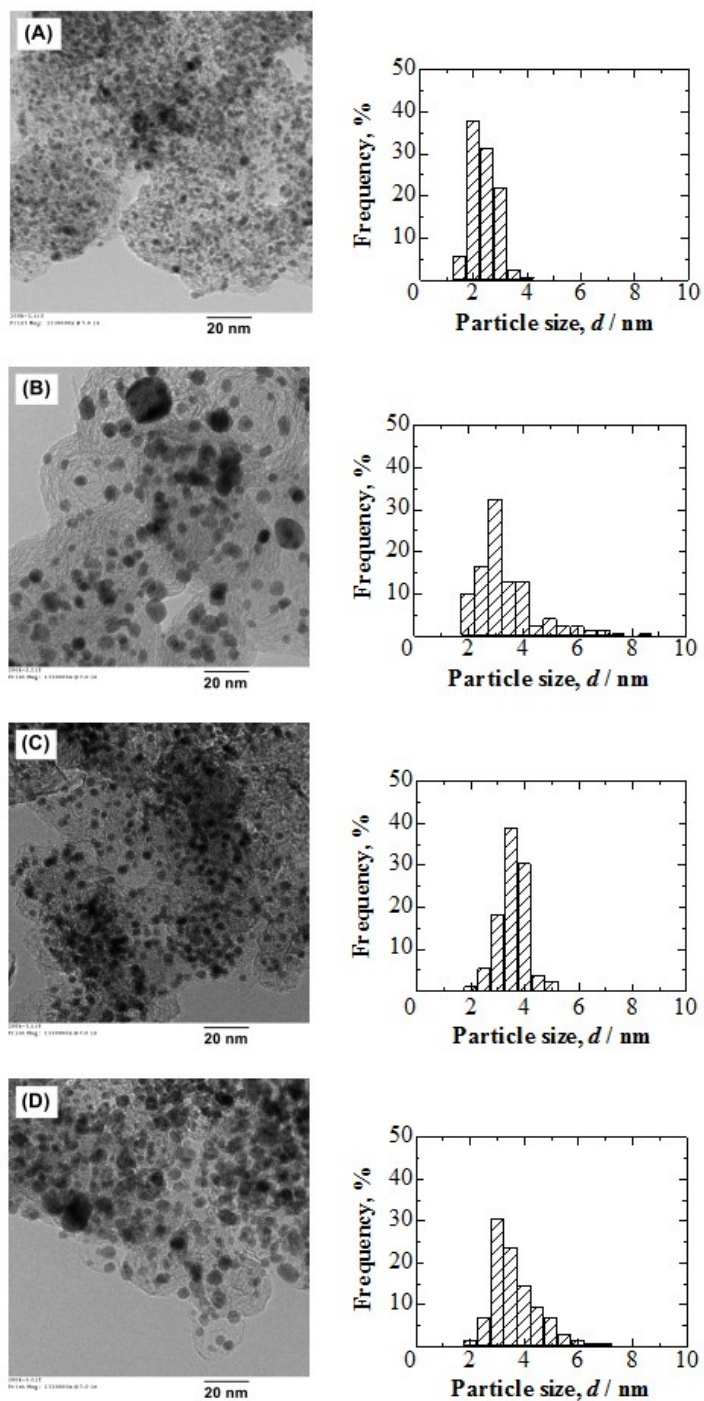


Figure S1. TEM images and particle size distribution histograms of (A) c-Pt/C, (B) c-Pt₃Co/C, (C) Pt₂AL-PtCo/C, and (D) c-Pt₂Ru₃/C catalysts.

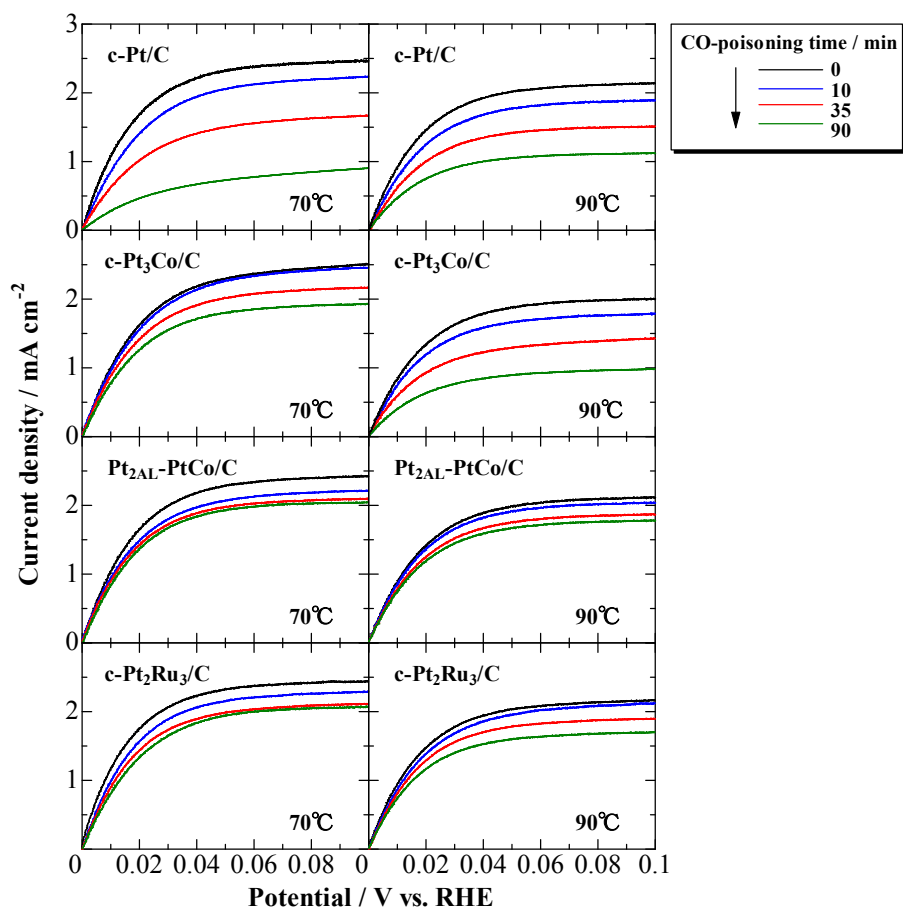


Figure S2. Hydrodynamic voltammograms for the HOR in H₂-saturated 0.1 M HClO₄ solution at Nafion-coated c-Pt/C, c-Pt₃Co/C, Pt_{2AL}-PtCo/C, and c-Pt₂Ru₃/C electrodes with various CO-poisoning time (1000 ppm CO/H₂) at 70°C and 90°C before recording CO-stripping voltammograms. The current densities are normalized to the real geometric area of the electrode. Potential scan rate = 1 mV s⁻¹. Mean flow rate of electrolyte $U_m = 18 \text{ cm s}^{-1}$.

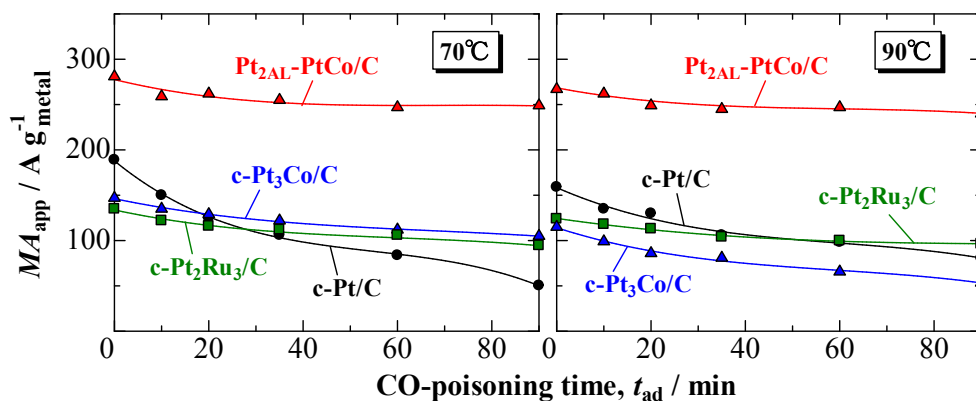


Figure S3. Change in the MA_{app} with CO-poisoning time (t_{ad}) for c-Pt/C, c-Pt₃Co/C, Pt_{2AL}-PtCo/C, and c-Pt₂Ru₃/C at 70°C and 90°C. After each electrode was exposed to 0.1 M HClO₄ solution saturated with 1000 ppm CO (H₂-balance) at 0.05 V for a given period t_{ad} , the MA_{app} was evaluated in H₂-saturated 0.1 M HClO₄ solution. We have noted that the MA_k in Table 1 showed that the c-Pt₂Ru₃/C was more active than the c-Pt₃Co/C, while in Figure S3 the MA_{app} of c-Pt₃Co/C seems to be slightly higher than that of c-Pt₂Ru₃/C at $\theta_{CO} = 0$ and 70 °C. We can check from the hydrodynamic voltammograms for the HOR at Nafion-coated c-Pt₃Co/C and c-Pt₂Ru₃/C electrodes at 70°C at $\theta_{CO} = 0$ (CO-poisoning time = 0) in Figure S2. There are two points that should be addressed for explanation: 1) The HOR current at 20 mV, I_{20mV} , for c-Pt₂Ru₃/C was about 1.02 times higher than that of c-Pt₃Co/C, whereas the metal mass was 1.07 times higher than that of c-Pt₃Co/C, and thus the MA_{app} (using the I_{20mV} divided by the metal mass) was smaller than that of c-Pt₃Co/C, as seen from Figure 1. 2) The I_k at 20 mV ($I_k = (I_L \times I_{20mV}) / (I_L - I_{20mV})$) for c-Pt₂Ru₃/C was about 1.15 times higher than that of c-Pt₃Co/C, and thus the MA_k (using the I_k divided by the metal mass) was still higher than that of c-Pt₃Co/C, as shown in Table 1. Generally, the difference is not so significant: the HOR activities are nearly identical.

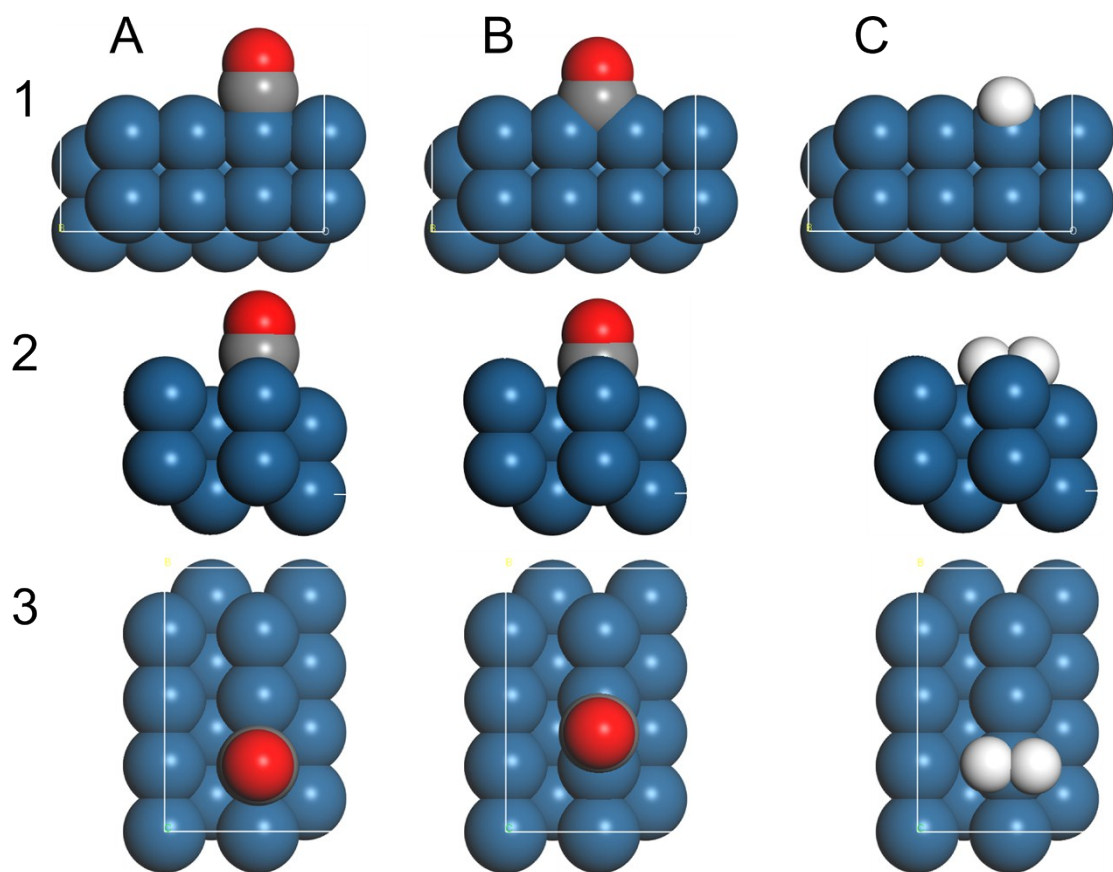


Figure S4. Pt(110) unit cells with (A) on-top CO, (B) bridging CO, and (C) on-top 2H; (1) cross-sectional view, (2) front view, and (3) top view.

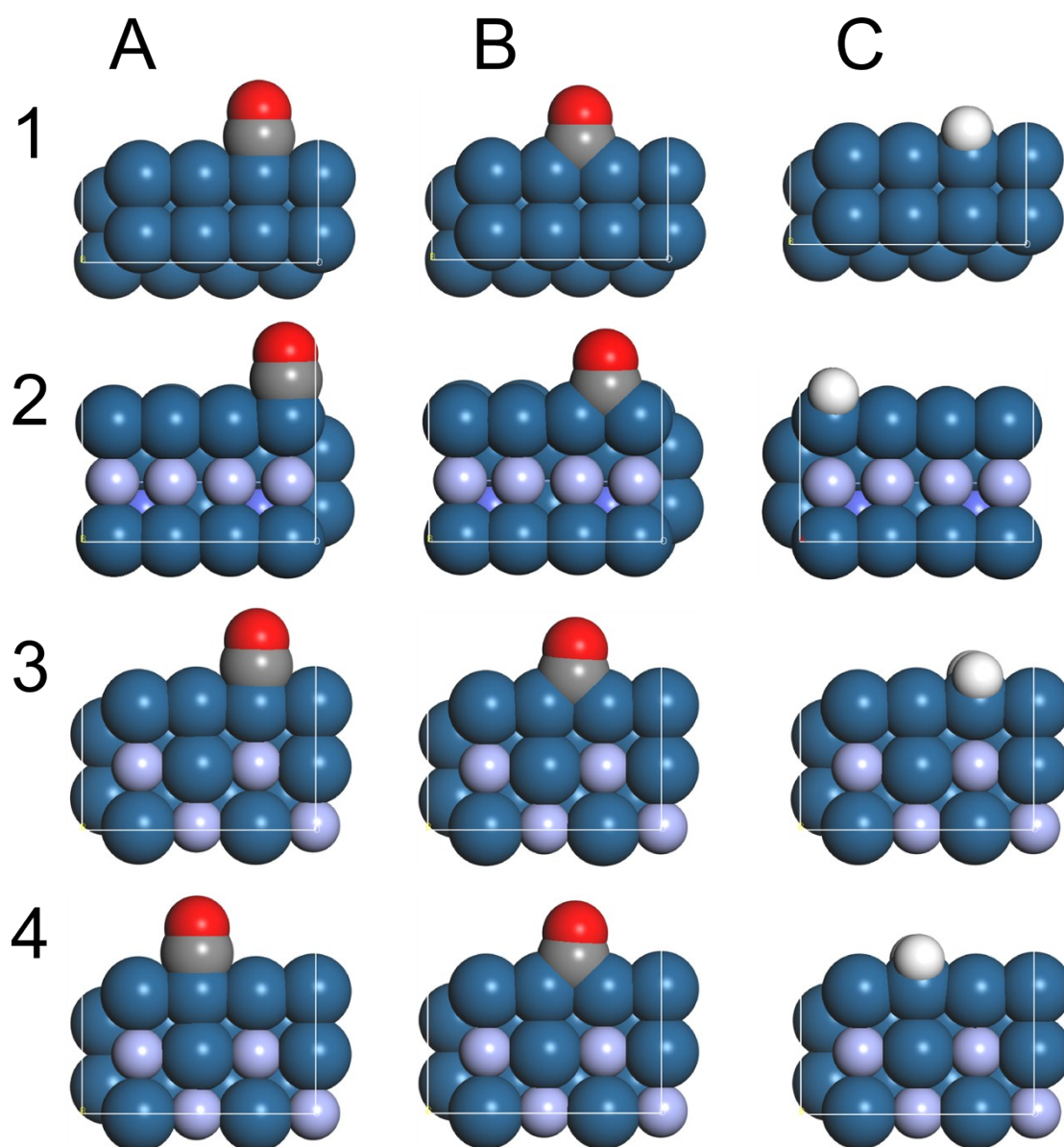


Figure S5. Cross-sectional views of unit cells with (A) on-top CO, (B) bridging CO, and (C) on-top (V-configuration) 2H adsorbates on the following surfaces: (1) Pt(110); (2) Pt skin/Pt₃Co(110) with enriched Co underlayer to simulate PtCo with two atomic layers of Pt skin; (3) Pt skin/Pt₃Co(110) with the on-top position situated above a Co atom in the second layer; and (4) Pt skin/Pt₃Co(110) with the on-top position situated above a Pt atom in the second layer. These images correspond to those in Fig. 2 in the main text.